27 March 1998

ELSEVIER

Chemical Physics Letters 285 (1998) 299–305

CHEMICAL PHYSICS LETTERS

Preparation of aligned carbon nanotubes catalysed by laser-etched cobalt thin films

M. Terrones [a,b], N. Grobert [a], J.P. Zhang [b], H. Terrones [c], J. Olivares [a], W.K. Hsu [a], J.P. Hare [a], A.K. Cheetham [b], H.W. Kroto [a], D.R.M. Walton [a]

[a] *School of Chemistry, Physics and Environmental Science, University of Sussex, Brighton BN1 9QJ, UK*
[b] *Materials Research Laboratory, University of California, Santa Barbara, CA 93106, USA*
[c] *Instituto de Física, UNAM, Apartado Postal 20-364, México D.F. 01000, México*

Received 18 December 1997; in final form 21 January 1998

Abstract

Pyrolysis of 2-amino-4,6-dichloro-s-triazine over laser-etched thin films of cobalt deposited on an inverted silica substrate generates aligned bundles and films of carbon nanotubes of uniform dimensions. Scanning electron microscopy, high resolution transmission electron microscopy, energy dispersive X-ray analyses, electron energy loss spectroscopy and electron diffraction studies reveal that the aligned tubes, which usually grow perpendicular to the substrate surface, are mainly straight (length $\leqslant 100$ μm; 30–50 nm OD), contain traces of nitrogen ($< 5\%$) and exhibit a preferred helicity (e.g. armchair 25–30%). Other graphitic structures (e.g. polyhedral particles, encapsulated particles and amorphous carbon) are absent. Energised cobalt clusters/particles ($\leqslant 50$ nm), ablated during laser-etching, may condense and recrystallise evenly on the surface of the substrate as cobalt and/or cobalt oxide. These crystals apparently play a key role in nanotube production. © 1998 Elsevier Science B.V.

1. Introduction

Soon after the identification of carbon nanotubes [1] in soot residues generated in the Krätschmer/Huffman fullerene reactor, bulk quantities were successfully prepared [2]. Nanotubes can now be produced from graphite by various techniques, including arc discharge [2–4], laser vaporisation [5–7] and electrolysis [8,9] and by hydrocarbon pyrolysis over catalysts [10–12].

Recent measurements on nanotubes [13,14], individual multi-layered tubes [15,16] and ropes of single-walled tubules [6] have revealed that their conducting properties depend markedly on the degree of graphitisation, helicity and diameter. Young's modulus measurements also show that multi-layered nanotubes are mechanically much stronger than conventional carbon fibres [17,18] and are extraordinarily flexible when subjected to substantial strain [19].

Most methods used, to date, to generate nanotubes suffer from the drawback that considerable quantities ($\leqslant 40\%$) of unwanted particles are also formed, although such particles can be eliminated by oxidation [20]. Unfortunately more than 95% of the nanotubes are also destroyed in this process and, to make matters worse, the remaining nanotubes lose their protective end-caps. As a result, further high temperature annealing (e.g. 3000 K) is necessary in order to eliminate dangling bonds located at the edges of the open nanotubes. Another general prob-

PII S0009-2614(98)00093-1

lem arises in that the dimensions of the nanotubes are highly variable. This Letter describes the production of aligned carbon nanotubes in high yield (uncontaminated by particles) of controlled length ($\leqslant$ 100 μm) and of fairly uniform external diameter (30–50 nm) by pyrolysis of 2-amino-4,6-dichloro-s-triazine over cobalt thin films, deposited on an inverted silica substrate, and etched using laser techniques. This method fosters the generation of small cobalt/cobalt oxide clusters of uniform size, which encourages the formation of the aligned tubes, crucial if the mechanical properties of the nanotubes as advanced composite materials are to be harnessed.

2. Experimental

2.1. Catalyst substrate.

A thin film of cobalt ($\approx$ 10–100 nm) was deposited on a silica plate (1 mm thick, 5 mm wide and 20 mm long) using laser ablation [21] and/or sublimation techniques. The plate was then exposed to air and etched with single laser pulses (Nd:YAG 266 nm; 5 mJ/pulse) using cylindrical lenses (65 mm focal length; Fig. 1a), thus creating linear tracks (width 1–20 mm; length $\leqslant$ 5 mm; Fig. 1b) where the cobalt had been ablated.

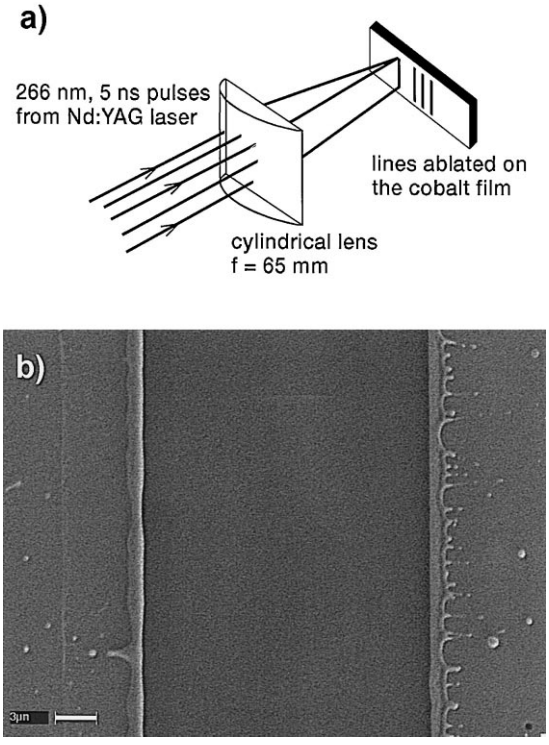

Fig. 1. (a) Etching technique using a Nd:YAG 266 nm laser and cylindrical lens (65 mm focal length). (b) SEM image from an etched nanotrack showing how uniform the channel is made. It is believed that along this channel/track uniform Co nanoparticles are deposited evenly by the laser striking the thin film.

2.2. Triazine preparation and pyrolysis

2-Amino-4,6-dichloro-s-triazine was prepared by modifying an existing procedure [22].

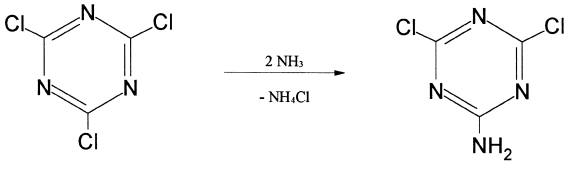

A solution of NH_3 (0.05 mol) in 1,4-dioxane (100 cm^3; Aldrich), was added dropwise to ice-cooled cyanuric chloride (4.6 g, 0.025 mol). The mixture was allowed to attain room temperature during 12 h (magnetic) stirring and was then heated to 95°C. Using a heated funnel, the solution was quickly filtered to remove precipitated NH_4Cl and then set aside to cool. Dioxane was removed under reduced pressure and the solid residue, 2-amino-4,6-dichloro-s-triazine, was recrystallised from hot water to constant mp 235°C dec (Ref. [22], 235°C), after removing final traces of water under high vacuum. ^{1}H-NMR ($CDCl_3$) δ 5.88 (s, 2H); MS (m/e) 164 (M^+).

2-Amino-4,6-dichloro-s-triazine (0.02–0.15 g) was introduced into one end of a silica tube (6 mm ID: length 60 cm), and the silica substrate coated with etched cobalt was placed facing *downwards* at the other end. The tube was then positioned in a two furnace system fitted with temperature controllers under an Ar flow (40 cm^3/min). Details of this pyrolytic process carried out at 950°C have been described elsewhere [21,23].

Following pyrolysis, the silica plate was covered with dark tracks observable to the naked eye; those areas where the cobalt film had not been laser-etched were transparent in most cases (see Section 2.1). Plates were analysed directly by scanning electron microscopy (SEM; Leo 5420 operated at 5–20 keV). The black deposits thereon were removed by scraping, dispersed in acetone, and analysed by transmission electron microscopy (TEM; JEOL JEM 100CX at 100 keV), high-resolution transmission electron microscopy (HRTEM; JEOL JEM 2010 at 200 keV and JEM 4000 at 400 keV), electron energy-loss spectroscopy (EELS; beam size 3 nm, 0.3 eV for fine dispersion study and 0.5eV for larger energy range with a collecting angle of 5 mrad for elemental ratio calculation) and energy dispersive X-ray (EDX; NORAN Instruments detector attached to the JEM 2010).

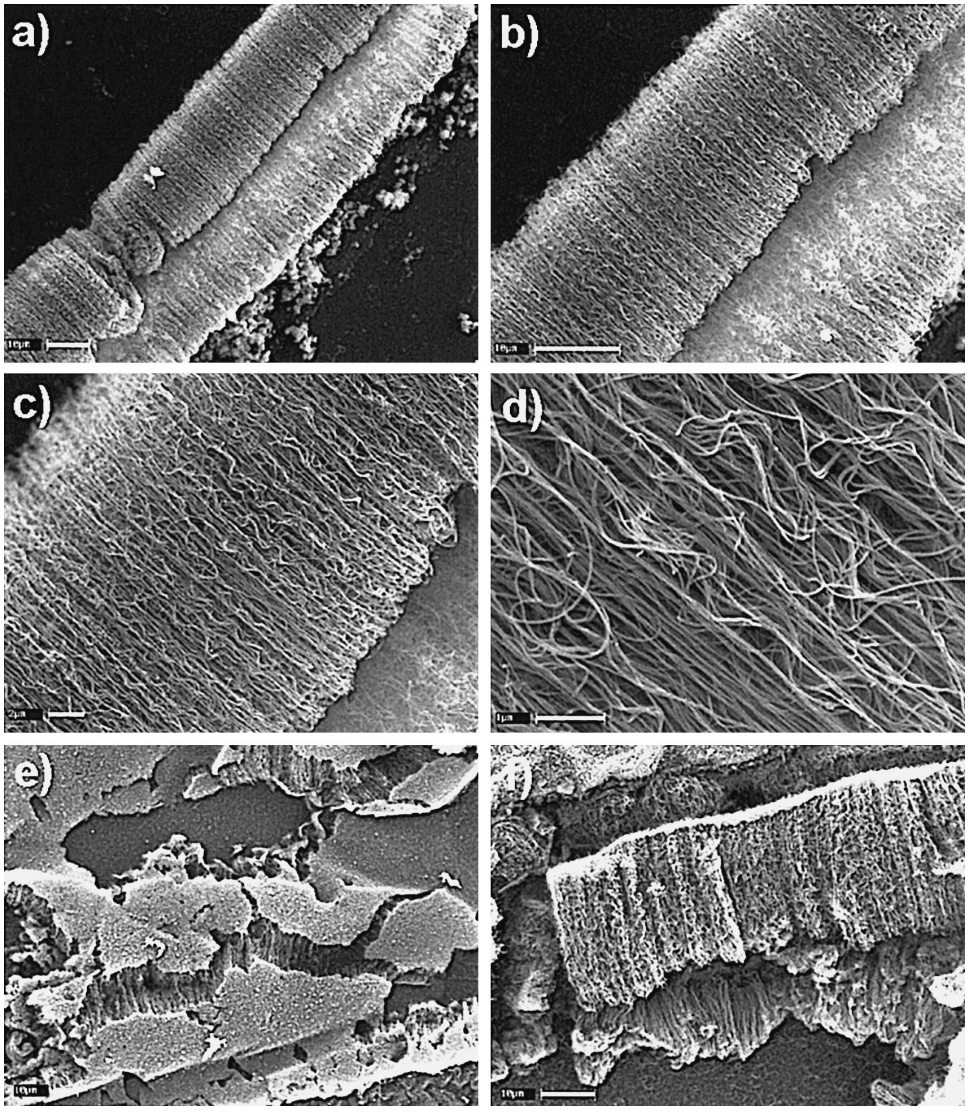

Fig. 2. SEM images of aligned nanotubes. (a) Double bundles at low magnification in which nanotubes appear aligned. (b–d) Higher magnification of these bundles showing aligned nanotubes exhibiting uniform lengths (20 μm) and diameters (30–50 nm). (e,f) Aligned nanotube films also generated in other substrates etched with different laser defocus conditions.

3. Results and discussion

3.1. Electron microscopy

SEM images show the presence of nanotube bundles closely aligned with the nanotracks (length 1–5 mm) created by laser etching (Fig. 2a–c,e). The tubes within these bundles were of uniform length ($\leqslant 100$ μm) and external diameter (≈ 30–50 nm; Fig. 2d). Probably as a result of the action of HCl, the cobalt thin film gradually disappeared from the plate during the experiment and appeared as cobalt dichloride (revealed by mass spectrometric analyses of the residues at the outlet bubblers) [21]. Interestingly, aligned nanotube films also were observed in other laser etched substrates using lower pulse energies out of focus (Fig. 2e,f). Related results have been observed previously [24–26].

TEM (Fig. 3a) and HRTEM observations confirm the presence of multi-layered graphitic tubes (30–50 nm OD 60–80 layers; Fig. 4). In most cases, cobalt ($\leqslant 50$ nm OD particles) was detected by EDX analysis within the nanotube tips (Fig. 3b). However, occasionally substantial sections of tubes were filled with cobalt (Fig. 4).

EELS analyses show that the nanotubes consist of carbon accompanied by traces of nitrogen ($< 5\%$; see Fig. 5a). In this context, it is possible that nitrogen, liberated during the cobalt catalysed triazine decomposition, is somehow trapped inside the hollow tubules. Alternatively, small C–N domains (sp^2 hybridised C–N regions < 5 nm OD) may have been generated within the tube walls (see Fig. 5b). However, no clear evidence for sp^2 hybridised nitrogen was found, except a broad and weak peak corresponding to the K-shell ionisation edge of nitrogen. Both EELS and EDX measurements indicate the absence of chlorine within the tubules.

Electron diffraction patterns [21] reveal a relatively well-ordered graphitic arrangement within the nanotubes, and that 25–30% of the tubes possess an armchair configuration (probably metallic [6]). This phenomenon may be due to preferential orientation of the cobalt or cobalt oxide clusters deposited along the laser-etched track. As mentioned previously [21], these clusters appear to be essential for tube growth, and subsequent axial carbon agglomeration, since tubules are not formed in the absence of the catalyst.

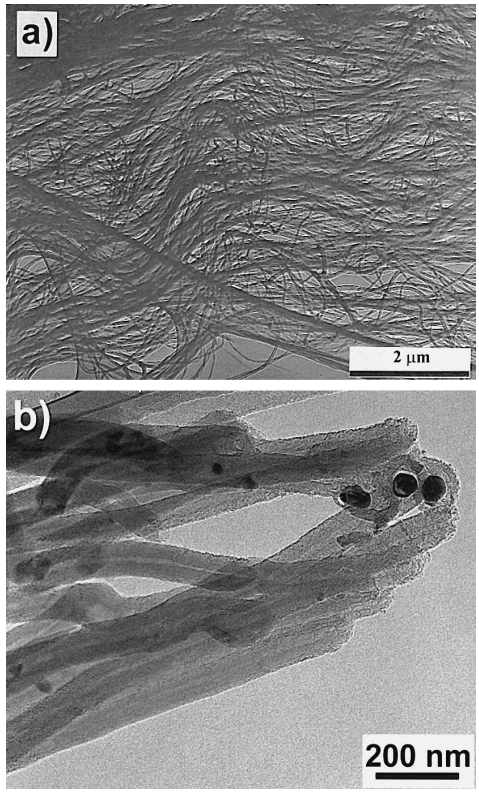

Fig. 3. (a) TEM image of a typical region filled with pure nanotubes. Polyhedral particles and other graphitic nanostructures are absent. (b) Low-resolution TEM image showing a group of parallel tubes together with three metal particles (< 40 nm OD) at the end of the bundle. These particles are lined up with the tube growth direction and are thought to be intimately responsible for the tubule formation. It is noteworthy that some nanotube tips do not contain a metal particle. This may because catalytic particles are located at a distance from the tips or, alternatively, are absent due to sonication (e.g. 30 min) damage of the structures.

3.2. Growth mechanism

Laser-etching of the cobalt thin film in air generates areas on the silica substrate free of cobalt. During this process, the energised cobalt clusters may condense and recrystalise as cobalt and/or cobalt oxide. It is possible that these clusters deposit evenly (with a preferred crystal orientation) along the edges of the eroded tracks. The clusters ($\leqslant 50$ nm) probably possess a large surface/volume ratio with excellent catalytic potential for nanotube growth (Fig. 3b).

A possible mechanism whereby aligned nanotubes

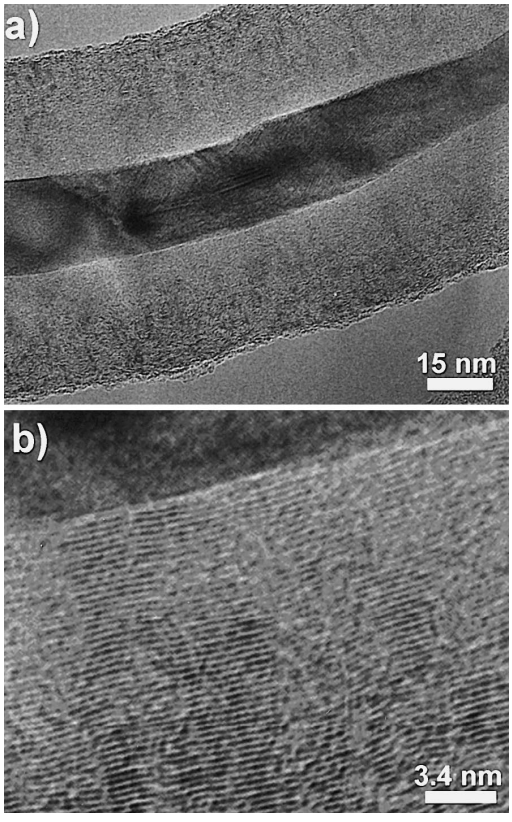

Fig. 4. (a) HRTEM image of a cobalt-filled nanotube, in which a cobalt–graphite interface from the nanotube shown in (b). The cobalt planes correspond to the (002) reflections separated by 2.35 Å. The simulation of the diffraction pattern with the (120) zone axis reproduces our observations of the cobalt planes.

grow over these etched regions may be rationalised as follows:

(1) 2-Amino-4,6-dichloro-s-triazine decomposes above 235°C liberating, in the first instance, HCl and triazine rings, which are transported in the Ar stream to the pyrolysis zone containing the inverted catalytic film at 950°C. At this point, HCl reacts with the smooth Co thin film, producing $CoCl_2$ in the gas phase. Almost simultaneously, the triazine rings, possibly fragment on the surface of the hot catalyst creating CN species.

(2) These CN units may fragment further, liberating gaseous N_2 and carbon. The carbon and possibly the nitrogen then precipitate on or diffuse *through* the metal clusters [27]. This process eventually results in axial nanotube growth. Temperature gradients occurring across the catalyst due to exothermic decomposition of the CN units may be a key factor. Nanotubes will continue to grow until the leading catalytic particle is deactivated or removed by the HCl.

(3) It is not clear at this stage why the nanotubes are aligned. It may be that, due to overcrowding, tubes grow simultaneously from the catalyst surface. Aligned nanotube growth only occurred when the experiment was conducted with the cobalt catalyst deposited on the lower (inverted) silica surface.

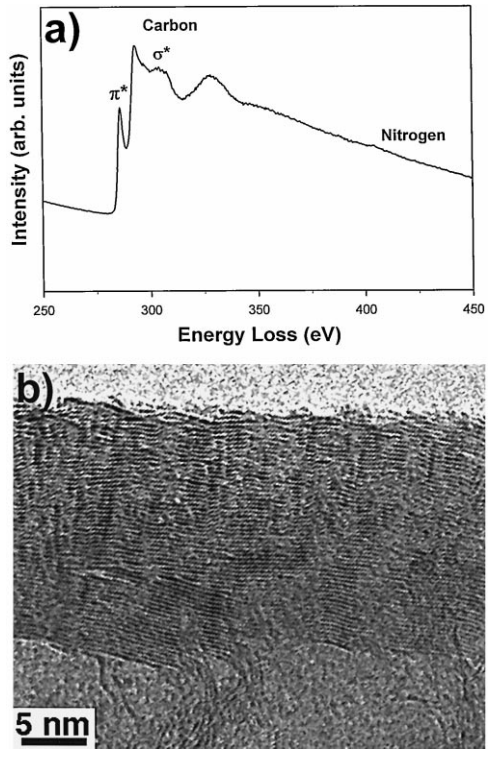

Fig. 5. (a) EELS spectra of a typical nanotube showing ionisation edges at ≈ 284 eV corresponding to the characteristic K-shell for carbon. The sharp peak at ≈ 284 eV is due to transitions from the 1s core level to the p* band and the intensity starting at ≈ 291 eV arises from transitions to the p-orbital of the s* band. Additionally, a weak and broad peak corresponds to the K-shell ionisation edge of nitrogen. The structure for this feature indicates the presence of traces of nitrogen (< 5%), possibly trapped within the tube during its formation. The dispersion per channel is 0.3 eV. (b) HRTEM image of a defecteive nanotube containing traces of nitrogen. The defective edges may consist of small C–N sp^2 regions within the hexagonal carbon network.

Growth of highly convoluted material was observed when the catalyst surface face upwards. It appears therefore that gravitational and convection effects may well be significant.

It should be noted that the size of the catalytic particles and the type of carbon source are crucial factors for nanotube production. In some cases, when the catalytic clusters are small, nanotube caps without encapsulated metal particles are found [24]. This phenomenon is uncommon when gaseous hydrocarbons are pyrolysed and may be associated with particle mobility during the tube growth process.

Recent pyrolysis experiments conducted with related precursors such as tris-aminotriazine (*melamine*) and cyanuric chloride over Co, Ni and Fe laser-etched thin films, also yielded similarly aligned nanotube bundles and films. The use of Fe films in conjunction with 2-amino-4,6-dichloro-s-triazine generated very long aligned nanotube bundles (< 250 μm, 20–40 nm OD) [24].

4. Conclusions

Laser etching of cobalt thin films provides a novel route to catalysts which, in conjunction with the pyrolysis of organic precursors (e.g. 2-amino-4,6-dichloro-s-triazine, etc.) yield to aligned nanotubes. These tubes are of uniform length ($\leqslant 100$ μm) and diameter (30–50 nm OD) and grow perpendicularly to the catalytic substrate *only* in the etched regions. The orientation of the catalytic particles ablated during etching appears to be crucial, nanotubes with preferred helicity being favoured. It is possible that matrices consisting of aligned nanotube bundles may be useful as novel mechanically strong composite materials and ultra-fine field emission sources [13,28–30].

Acknowledgements

We thank K. Kordatos for the supply of 2-amino-4,6-dichloro-s-triazine. We are grateful to R. Guardián, R. Hernández, P. Mexia, K. Prassides, D.P. Randall, L. Rendón, S. Tehuacanero, J. Thorpe, and P.D. Townsend for useful discussions and for providing Electron Microscope facilities. We thank the Royal Society (London), BOC gases, the DERA (NG), CONACYT-México (HT), DGAPA-UNAM IN 107-296 (HT), EU-TMR grant (JO) and the EPSRC for financial support.

References

[1] S. Iijima, Nature 354 (1991) 56.
[2] T.W. Ebbesen, P.M. Ajayan, Nature 358 (1992) 220.
[3] S. Iijima, P.M. Ajayan, T. Ichihashi, Phys. Rev. Lett. 69 (1992) 3100.
[4] T.W. Ebbesen, Annu. Rev. Mater. Sci. 24 (1994) 235.
[5] T. Guo, P. Nikoleav, A.G. Rinzler, D. Tománek, D.T. Colbert, R.E. Smalley, J. Phys. Chem. 99 (1995) 10694.
[6] A. Thess, R. Lee, P. Nikolaev, H. Dai, P. Petit, J. Robert, C. Xu, Y.H. Lee, S.G. Kim, A.G. Rinzler, D.T. Colbert, G.E. Scuseria, D. Tománek, J.E. Fischer, R.E. Smalley, Science 273 (1996) 483.
[7] L.C. Qin, S. Iijima, Chem. Phys. Lett. 269 (1997) 65.
[8] W.K. Hsu, J.P. Hare, M. Terrones, P.J.F. Harris, H.W. Kroto, D.R.M. Walton, Nature 377 (1995) 687.
[9] W.K. Hsu, M. Terrones, J.P. Hare, H. Terrones, H.W. Kroto, D.R.M. Walton, Chem. Phys. Lett. 261 (1996) 161.
[10] M. Endo, K. Takeuchi, K. Kobori, K. Takahashi, H.W. Kroto, A. Sarkar, Carbon 33 (1995) 873.
[11] S. Amelinckx, X.B. Zhang, D. Bernaerts, X.F. Zhang, V. Ivanov, J.B. Nagy, Science 265 (1994) 635.
[12] D. Bernaerts, X.B. Zhang, X.F. Zhang, S. Amelinckx, G. Van Tendeloo, J. Van Landuyt, V. Ivanov, J.B. Nagy, Phil. Mag. A 71 (1995) 605.
[13] W.A. De Heer, A. Chatelain, D. Ugarte, Science 270 (1995) 1179.
[14] M. Terrones, J.P. Hare, W.K. Hsu, H.W. Kroto, A. Lappas, W.K. Maser, A.J. Pierik, K. Prassides, R. Taylor, D.R.M. Walton, in: K.M. Kadish, R.S. Ruoff (Eds.), Recent Advances in the Chemistry and Physics of Fullerenes and Related Materials, Vol. 2 (Electrochemical Society, Pennington, NJ, 1995), p. 599.
[15] H.J. Dai, E.W. Wong, C.M. Lieber, Science 272 (1996) 523.
[16] T.W. Ebbesen, H.J. Lezec, H. Hiura, J.W. Bennett, H.F. Ghaemi, T. Thio, Nature 382 (1996) 54.
[17] M.J. Treacy, T.W. Ebbesen, J.M. Gibson, Nature 381 (1996) 678.
[18] E.W. Wong, P.E. Sheehan, C.M. Lieber, Science 277 (1997) 1971.
[19] M.R. Falvo, G.J. Clary, R.M. Taylor II, V. Chi, F.P. Brooks Jr, S. Washburn, R. Superfine, Nature 389 (1997) 582.
[20] T.W. Ebbesen, P.M. Ajayan, H. Hiura, K. Tanigaki, Nature 367 (1994) 519.
[21] M. Terrones, N. Grobert, J. Olivares, J.P. Zhang, H. Terrones, K. Kordatos, W.K. Hsu, J.P. Hare, P.D. Townsend, K. Prassides, A.K. Cheetham, H.W. Kroto, D.R.M. Walton, Nature 388 (1997) 52.

[22] J.T. Thurston, J.R. Dudley, D.W. Kaiser, I. Hechenbleikner, F.C. Schaefer, D. Holm-Hansen, J. Am. Chem. Soc. 73 (1951) 2981.
[23] M. Terrones, A.M. Benito, C. Manteca-Diego, W.K. Hsu, O.I. Osman, J.P. Hare, D.G. Reid, H. Terrones, A.K. Cheetham, K. Prassides, H.W. Kroto, D.R.M. Walton, Chem. Phys. Lett. 257 (1996) 576.
[24] N. Grobert, S. Trasobares, M. Terrones, H. Terrones, W.K. Hsu, A.K. Cheetham, J.P. Zhang, H.W. Kroto, D.R.M. Walton, manuscript in preparation.
[25] W.Z. Li, S.S. Xie, L.X. Qian, B.H. Chang, B.S. Zou, W.Y. Zhou, R.A. Zhao, G. Wang, Science 274 (1996) 1701.
[26] Y. Chen, Z.L. Wang, J.S. Yin, D.J. Johnson, R.H. Prince, Chem. Phys. Lett. 272 (1997) 178.
[27] R.T.K. Baker, Carbon 27 (1989) 315.
[28] A.G. Rinzler, J.H. Hafner, P. Nikolaev, L. Lou, S.G. Kim, D. Tomànek, P. Nordlander, D.T. Colbert, R.E. Smalley, Science 269 (1995) 1550.
[29] P.G. Collins, A. Zettl, Appl. Phys. Lett. 69 (1996) 1969.
[30] Y. Saito, K. Hamaguchi, K. Hata, K. Uchida, Y. Tasaka, F. Ikazaki, M. Yumura, A. Kasuya, Y. Nishima, Nature 389 (1997) 555.